iJRASET
International Journal For Research in Applied Science and Engineering Technology

# INTERNATIONAL JOURNAL FOR RESEARCH

IN APPLIED SCIENCE & ENGINEERING TECHNOLOGY

**Volume:** 7 **Issue:** VI **Month of publication:** June 2019

**DOI:** http://doi.org/10.22214/ijraset.2019.6413

www.ijraset.com

Call: 08813907089 | E-mail ID: ijraset@gmail.com

International Journal for Research in Applied Science & Engineering Technology (IJRASET)
*ISSN: 2321-9653; IC Value: 45.98; SJ Impact Factor: 7.177*
*Volume 7 Issue VI, June 2019- Available at www.ijraset.com*

# Flexural and Distortional Deformations of Composite and Non-Composite Thin-Walled Box Girder Structures

Chidolue Chinenye A[1], Ngele Celestine F[2]
[1, 2]*Department of Civil Engineering, Faculty of Engineering Nnamdi Azikiwe University, Awka, Anambra State, Nigeria.*

***Abstract:*** ***The high torsional stiffness of box girders makes them popular in modern bridge structures. However, the thinness of their cross section predisposes them to a complex structural behaviour. All thin walled structures resist eccentric vertical load in bending action and torsion. The torsional component of the eccentric load gives rise to pure torsion (Saint Venant torsion), and warping torsion (distortion), in addition to flexure in the non-symmetric axis of the structure. A better understanding of the complex interactions between these strain modes, is necessary for predicting the behavior of such structures under generalized loading. This paper studied the interaction between the flexural and distortional strain modes of thin-walled mono-symmetric, composite and non-composite box girder sections using Vlasov's theory of thin-walled structures. The stain mode diagrams for the study sections were drawn, and used to evaluate the Vlasov's coefficients. The loading on the girders was computed using the British Standard Specification for Highway Bridge Live Loads (BS5400-2-2006). The general differential equations of equilibrium for flexural-distortional analysis of a mono-symmetric box girder sections were used to analyse and compare the flexural and distortional deformations of the composite and non-composite sections. The results show that the non-composite section is better in resisting flexural and distortional loads than the composite section.***
***Keywords: Composite, Uniform, Distortion, flexure, thin walled box girder, Vlasov's theory.***

## I. INTRODUCTION

A composite thin walled structure is one in which two or more materials are combined in a visible form, while a uniform structural system is homogenous in its material composition. Composites are primarily attractive because of their high strength-to-weight, and stiffness-to-weight ratios, [1]. Composite mono-symmetric box girders are increasingly being used in highway construction works, such as bridge of various types, grade separated intersections, etc. The arrangement of materials in a composite structure can appear in many forms, but this paper considered an arrangement whereby the top and bottom flanges are made of concrete while the webs are made of steel as shown in Fig.1(a).

## II. SECTION TRANSFORMATION IN COMPOSITE MEMBERS

For compatibility in the concrete-steel girder, the flexural rigidity of the composite members will be equal. Considering a unit width of concrete ($b_c$) and steel($b_s$) sections, thickness of concrete section ( $t_c$ = 200mm) and noting that the Young's modulus of grade 42 concrete is 35kN/mm$^2$, [2] while that of steel is 200kN/mm$^2$, [3]. Then compatibility requires that rigidity of concrete and steel plates be equal and one can obtain the thickness of steel section ($t_s$). Thus,

$$E_c I_c = E_s I_s \qquad (2.0)$$

$$\frac{E_c b_c t_c^3}{12} = \frac{E_s b_s t_s^3}{12} \qquad (2.1)$$

$$\frac{35 \times 1000 \times 200^3}{12} = \frac{200 \times 1000 \times t_s^3}{12}$$

:. $t_s$ = 112mm, assuming thickness of steel webs =112mm

Fig.1a presents the composite study section, while
Fig.1b presents the non-composite study section.

*ISSN: 2321-9653; IC Value: 45.98; SJ Impact Factor: 7.177*
*Volume 7 Issue VI, June 2019- Available at www.ijraset.com*

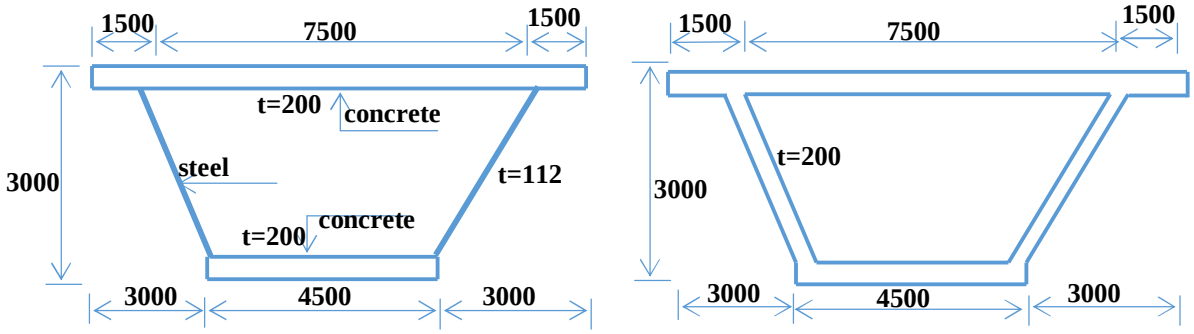


(a)Single cell composite box girder section (b)Single cell uniform concrete box girder section

Fig.1; Composite and non-composite box girder sections

## III. LITERATURE REVIEW

Many researchers, [4], [5], [6], [7], and [8], undertook experimental and theoretical studies to better understand the shear behaviour of composite box girder structures. Based on the analysis carried out to date, it has been established that shear forces are mostly resisted by corrugated steel web.

Gupta et al [9], used finite element formulations to study the behaviour of composite box girder bridge. They considered deflections, longitudinal and transverse bending stresses. Sayed [10], studied the lateral torsional buckling of steel I-girder with corrugated steel web using numerical analysis. He compared his results with girder made with plane web.

Some other literatures, [11], [12], and [13], on open and closed composite thin-walled beams, dealt with analytical formulations on the distribution of warping stresses and location of shear center of such complex structural system. Few others; [14], and [15], however centered on stability analysis of composite box girders using experimental and finite element formulations, considering initial imperfections and shear deformation of the composite box girder in their analysis. Osadebe and Chidolue [16],[17], obtained fourth order differential equations of torsional-distortional equilibrium, and flexural-distortional equilibrium for the analysis of mono-symmetric box girder structures using Vlasov theory with modification by Varbanov [18].

Through experimental and analytical means, various researchers have put forward various theories examining methods of analysis, both numerical and classical. Vlasov theory was however adjudged to contain all peculiarities of cross sectional deformations, such as warping, torsion, distortion, etc. and is therefore adopted in this work.

## IV. VLASOV'S STRESS-STRAIN RELATIONS

The Vlasov's stress-stain relation which forms the bases for the formulation of the governing equations of flexural-distortional equilibrium are shown below;

Generally, strain is given by;

$$\varepsilon = \frac{\Delta l}{l} \qquad (1)$$

Where, $\Delta l$ *is the* elongation, l, is the original length, and $\varepsilon$, *is the strain*.

Let the elongation in the longitudinal and transverse direction of an infinitesimal length dx, be, $\partial u(x,s)$ and $\partial v(x,s)$ respectively.

From the theory of elasticity, the strains in the longitudinal and transverse directions are given by;

$$\frac{\partial u(x,s)}{\partial x} = \sum_{i=1}^{m} U_i'(x)\varphi k(s) \quad \text{and}$$

$$\frac{\partial v(x,s)}{\partial x} = \sum_{k=1}^{n} V_k'(x)\psi k(s) \qquad (2)$$

The expression for shear strain is

$$\gamma(x,s) = \frac{\partial u}{\partial z} + \frac{\partial v}{\partial x} \quad (3)$$

And in series form we have,

$$\gamma(x,s) = \sum_{i=1}^{m} \varphi i(s) Ui(x) + \sum_{i=1}^{n} \psi k(s) V'_k(x) \quad (4)$$

Using the above displacement fields and basic stress-stain relationships of the theory of elasticity, the expressions for normal and shear stresses become:

$$\sigma(x,s) = E\frac{\partial u(x,s)}{\partial x} = E\sum_{i=1}^{m} \varphi i(s) U'_i(x) \quad (5)$$

$$\tau(x,s) = G\gamma(x,s) = G\left[\sum_{i=1}^{m} \varphi'_i(s) Ui(x) + \sum_{k=1}^{n} \psi k(s) V'_k(x)\right] \quad (6)$$

Where, U(x) and V(x) are unknown functions governing the displacements in the longitudinal and transverse directions respectively. φi(s) and ψk(s) are elementary displacements of the strip frame, respectively out of the plane (m displacement) and in the plane (n displacements). These displacements are chosen among all displacements possible, and are called the generalized strain co-ordinates of a strip frame.

Transverse bending moment generated in the box structure due to distortion is given by

$$M(x,s) = \sum_{k=1}^{n} m_k(s) v_k(x) \quad (7)$$

Where $m_k(s)$ is the bending moment generated in the cross sectional frame due to a unit distortion,( V(x) = 1), [21].

## V. FLEXURAL-DISTORTIONAL EQUILIBRIUM EQUATIONS.

Osadebe and Chidolue [16],[17], derive the following equilibrium equations for flexural-distortional analysis of a mono-symmetric box girder section.

$$ka_{22}U_2^{IV} + ka_{23}U_3^{IV} - b_{22}u_2 - C_{22}V_2'' - C_{23}V_3'' = 0 \quad (8a)$$

$$ka_{32}U_2^{IV} + ka_{33}U_3^{IV} - b_{32}u_2 - b_{33}U_3 - C_{32}V_2' - C_{33}V_3' = 0 \quad (8b)$$

$$C_{22}U_2' + C_{23}U_3' + \gamma_{22}V_2^{IV} + \gamma_{23}V_3^{IV} = \frac{-q_2}{G} \quad (8c)$$

$$C_{32}U_2' + C_{33}U_3' + KS_{33}V_3 + \gamma_{32}V_2^{IV} + \gamma_{33}V_3^{IV} = \frac{-q_3}{G}. \quad (8d)$$

Where $a_{ij}$, $b_{ij}$, $c_{ij}$, and $r_{ij}$ are Vlasov's coefficients, obtained by diagram multiplication of the strain modes diagrams, while $s_{hk}$ is obtained by diagram multiplication of the distortional bending moment diagram.

$$a_{ij} = a_{ji} = \int \varphi i(s)\varphi j(s)\,dA$$

$$b_{ij} = b_{ji} = \int \varphi'_i(s)\varphi''_i(s)\,dA$$

$$c_{jk} = c_{kj} = \int \varphi'_k(s)\psi j(s)\,dA$$

$$c_{ik} = c_{ki} = \int \varphi'_i(s)\psi k(s)\,dA \quad (9)$$

$$r_{kk} = r_{kk} = \int \psi k(s)\psi_k(s)\,dA$$

$$q_k = \int q\,\psi_k\,ds \quad (10)$$

Simplifying eqns.8, by elimination of $U_2$ , $U_3$ and their derivatives, we obtain;

$$\alpha_1 V_2^{IV} + \alpha_2 V_3^{IV} - \beta_1 V_3'' = K_3 \quad (11)$$

$$\alpha_3 V_2^{IV} + \alpha_4 V_3^{IV} - \beta_2 V_3'' - \gamma_1 V_3 = -K_4 \quad (12)$$

Below are the expressions for the coefficients of the equilibrium equations (eqns. 11 and 12).

$\alpha_1 = ka_{22}$ (a)

$\alpha_2 = ka_{23}$ (b)

$\alpha_3 = ka_{32}$ (c)

$\alpha_4 = ka_{33}$ (d)

$$\beta_1 = \left(\frac{k^2 s_{33}(a_{33}c_{22} - a_{32}c_{23})}{c_{33}c_{22} - c_{32}^2}\right) \quad \text{(e)}$$

$$\beta_2 = \left(\frac{k^2 s_{33}(a_{33}c_{22} - a_{32}c_{23})}{c_{33}c_{22} - c_{32}^2}\right) \quad \text{(f)}$$

$$\eta_1 = \left(\frac{k s_{33}(b_{32}c_{23} - b_{33}c_{22})}{c_{33}c_{22} - c_{32}^2}\right) \quad \text{(g)}$$

$$K_1 = \left(\frac{c_{32}}{c_{33}c_{22} - c_{32}^2}\right)\frac{q_2}{G} - \left(\frac{c_{22}}{c_{33}c_{22} - c_{32}^2}\right) \quad \text{(h)}$$

$$K_2 = \left(\frac{c_{23}}{c_{33}c_{22} - c_{32}^2}\right)\frac{q_3}{G} - \frac{q_2}{c_{22}G} - \left(\frac{c_{32}}{c_{33}c_{22} - c_{32}^2}\right)\frac{c_{23}q_2}{c_{22}G}$$

(i)

$$K_3 = b_{22}k_1 - b_{22}K_2 \quad \text{(j)}$$

$$K_4 = b_{32}K_2 + b_{33}K_1 \quad \text{(k)} \qquad (13)$$

Equations 11 and 12 are coupled with respect to $V_2$ and $V_3$, showing that there is interaction between minor axis flexural displacement, $V_2$, and distortional displacement, $V_3$, at the axis of un-symmetry. Hence the two equations can be solved simultaneously. Equations 11 and 12 are the differential equations of equilibrium for flexural-distortional analysis of a mono-symmetric box girder section based on Vlasov's theory.

## VI. STRAIN MODES DIAGRAMS FOR COMPUTATION OF VLASOV'S COEFFICIENTS.

Figures 2a and 3a show the cross sections of the study profiles. Figs.2 (b to h) and Figs.3 (b to h) show the generalized strain modes diagrams for the composite and the uniform sections respectively.

$\varphi_1$ (Fig 2c) is a property of the cross section obtained by plotting the displacement of the members of the cross section when the vertical (z-z) axis is rotated through a unit radian, similarly, $\varphi_2$ (Fig 2e) is a property of the cross section obtained by plotting the displacement of the members of the cross section when the horizontal (y-y) axis is rotated through a unit radian. The warping function $\varphi_3$(Fig 2g) of the box cross section is obtained as detailed in literatures: [21], [16], [17]. $\psi_1, \psi_2$ are in plane displacements of the cross section in x-z and x-y planes respectively. $\psi_3$ is the distortion diagram for the cross section which is obtained by differentiation of the warping function diagram, $\varphi_3$. $\psi_4$(Fig2b) is the displacement diagram for the box girder cross section when the frame is rotated one radian in say, a clockwise direction about the centroidal axis. Thus, $\psi_4$ is directly proportional to the perpendicular distance (radius of rotation), from the centroidal axis to the members of the cross section.

Osadebe and Chidolue [16]) showed that the in plane displacements of the cross section; $\psi_1, \psi_2, and\ \psi_3$ are the same as the derivatives of their out of plane displacements. Consequently, $\psi_1, \psi_2, and\ \psi_3$ are obtained by numerical differentiation of $\varphi_1, \varphi_2$ and $\varphi_3$ diagrams respectively.

International Journal for Research in Applied Science & Engineering Technology (IJRASET)
*ISSN: 2321-9653; IC Value: 45.98; SJ Impact Factor: 7.177*
*Volume 7 Issue VI, June 2019- Available at www.ijraset.com*

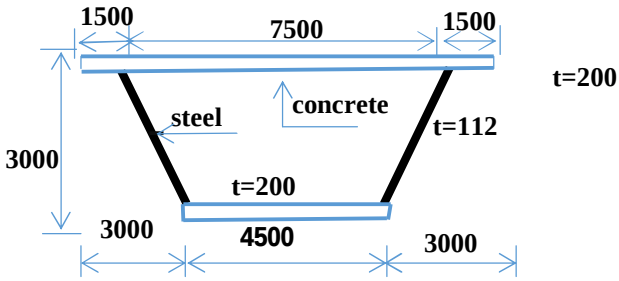


(a) Single cell composite box girder section

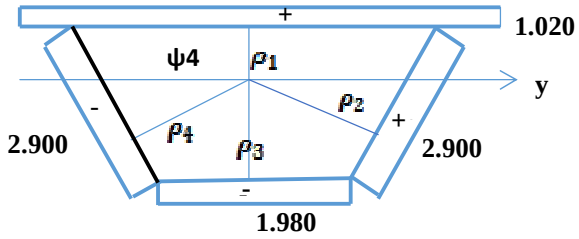


(b) Pure rotation diagram; $\psi_4$

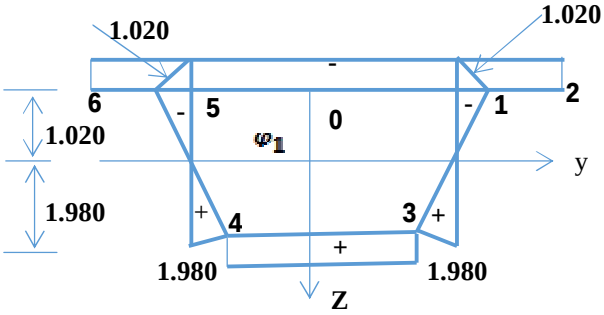


© Longitudinal strain mode diagram (bending in y-y axis)

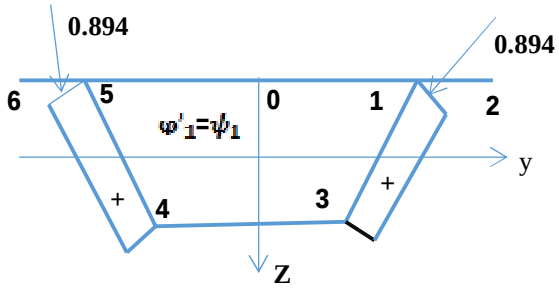


(d) Transverse strain mode in y-direction

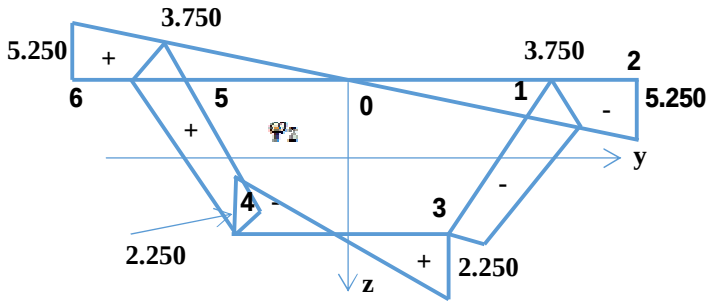


(e) Longitudinal strain mode diagram (bending about z-z axis)

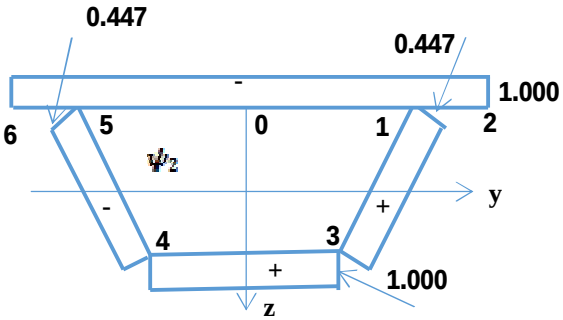


(f) Transverse strain mode in z- direction

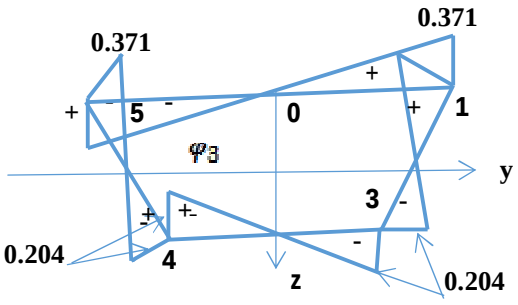


(g) Warping function

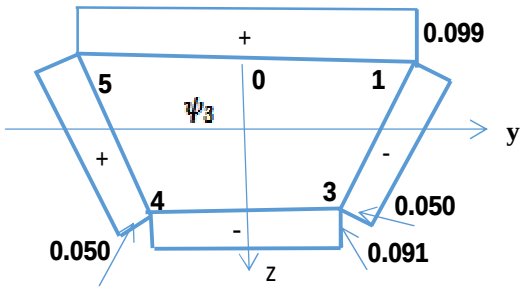


(h) Distortion diagram

Fig.2: Generalized strain modes diagram for the composite section

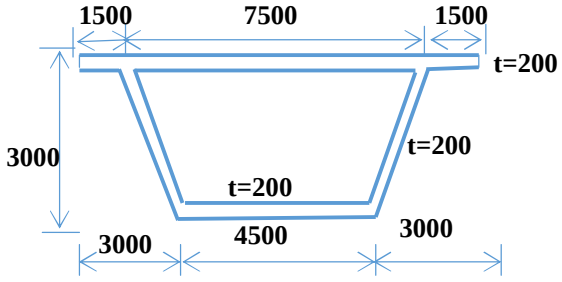


(b) Single cell box girder section

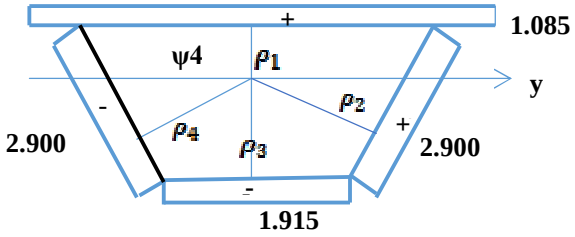


(b) Pure rotation diagram

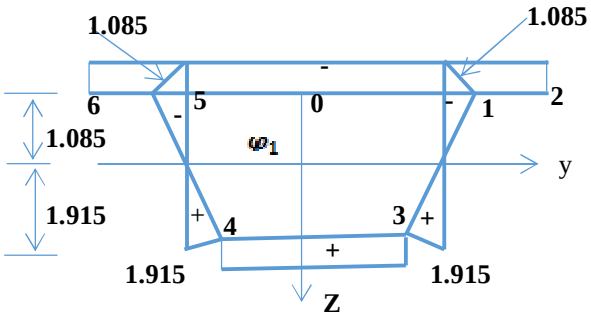


© Longitudinal strain mode diagram (bending in y-y )axis)

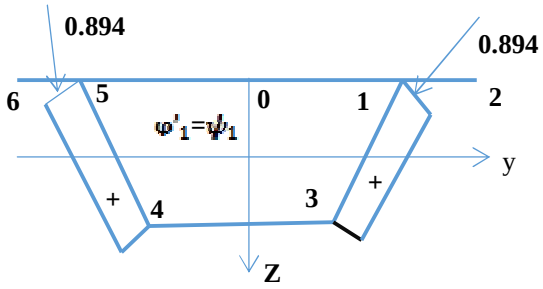


(d) Transverse strain mode in y-direction

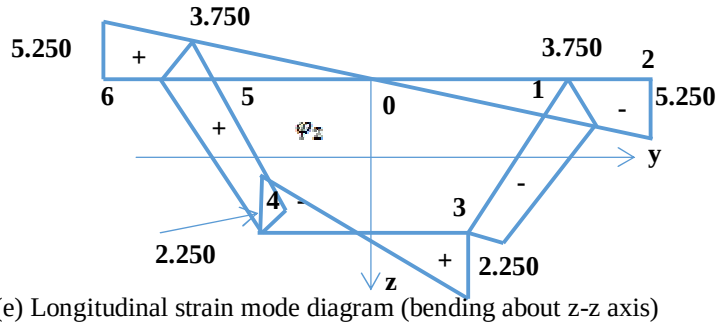


(e) Longitudinal strain mode diagram (bending about z-z axis)

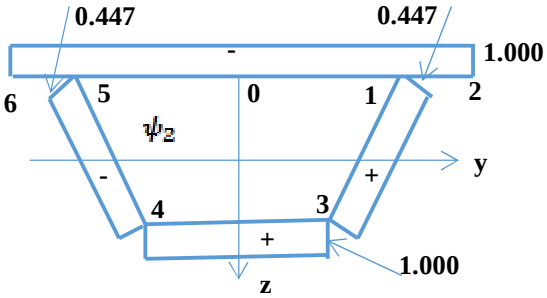


(f) Transverse strain mode in z- direction

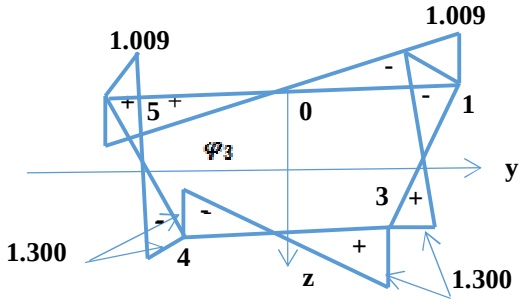


(g) Warping function diagram

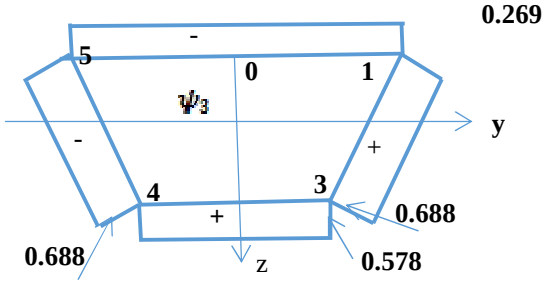


(h) Distortion diagram

Fig.3: Generalized strain modes diagram for the uniform concrete section

International Journal for Research in Applied Science & Engineering Technology (IJRASET)
*ISSN: 2321-9653; IC Value: 45.98; SJ Impact Factor: 7.177*
*Volume 7 Issue VI, June 2019- Available at www.ijraset.com*

## VII.DISTORTIONAL BENDING MOMENT DIAGRAM, M(S);

The distortional bending moment diagram was obtained from the warping function diagram, which was differentiated to obtain the distortion diagram shown in Fig.4a. In line with the directional movement of the plate elements in the distortion diagram, a base system for evaluation of distortional bending moment of the box frames were drawn. Fig.4b shows the base system for the composite section. A unit rotation,( $x_i = 1$) and a unit translation,( $R_i = 1$) are applied at the joints of the frame, the effects of which are summed up to obtain the distortional bending moment diagram according to eqn.(14) below,

$$M_k(s) = \sum m_i x_i + \sum m_i R_i \Delta_i \qquad (14)$$

Where $\sum m_i x_i$ and $\sum R_i \Delta_i$ are work done on the plates due to unit rotation and unit translation at the joints respectively, Rekach([21].

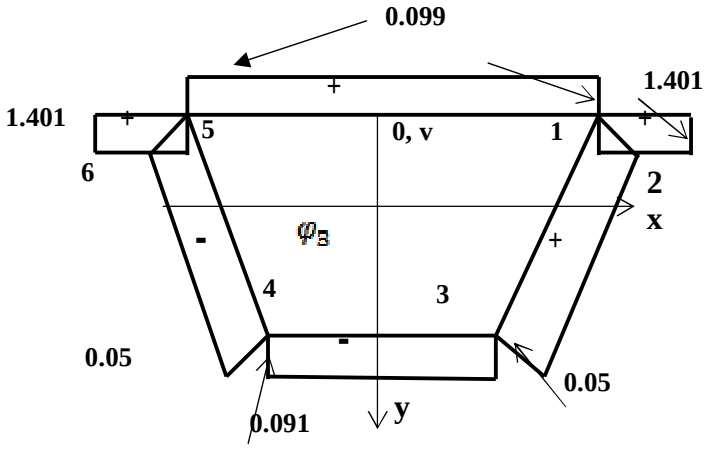


Fig 4 a: Distortion diagram for the composite section

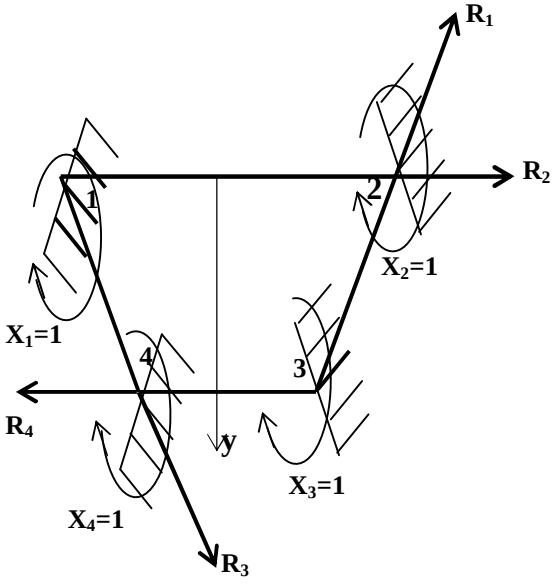


Fig 4b: Base system for the composite section

*ISSN: 2321-9653; IC Value: 45.98; SJ Impact Factor: 7.177*
*Volume 7 Issue VI, June 2019- Available at www.ijraset.com*

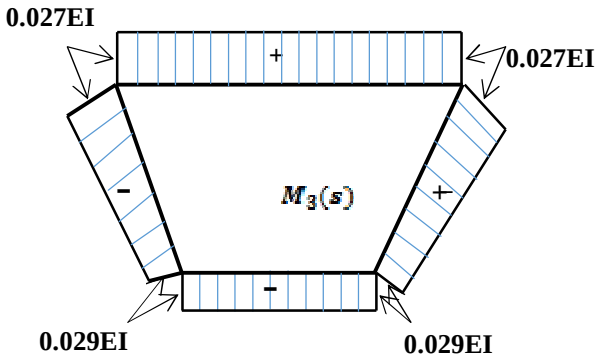


Fig 5a: Distortional bending moment diagram for the composite section.

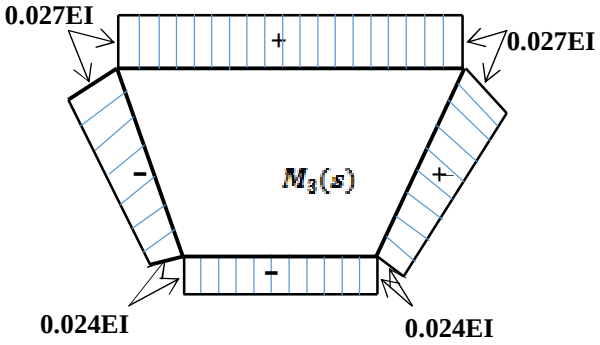


Fig 5b: Distortional bending moment diagram for the uniform concrete section.

*A. The $S_{hk}$ coefficients,*

The coefficient $S_{hk}$ given by eqn.(14), depends on the bending deformation of the strip frame characterized by $M_k$ ( for k = 1, 2, 3, 4 ). To compute the coefficient, the bending moment diagrams due to the strain modes $\psi_1, \psi_2, \psi_3, and\ \psi_4$, would be needed. Incidentally, strain modes $\psi_1, \psi_2, and\ \psi_4$ do not generate distortional bending moment, as they involve pure bending and pure rotation. Only strain mode $\psi_3$ generates distortional bending moment which can be evaluated using the distortion diagram, Figs.2(h). and 3(h). The relevant expression for the coefficient is given by;

$$S_{hk}=S_{kh}=\frac{1}{E}\int \frac{M_h(s)M_k(s)}{E1(s)}ds \qquad (15)$$

Where $M_3$ is the distortional bending moment of the cross section obtained as described earlier. Having obtained the distortional bending moment, $M_3$ ,the coefficient $S_{hk}$ is obtained using the Mohr integral for displacement computation(diagram multiplication) of the bending moment diagram.

*ISSN: 2321-9653; IC Value: 45.98; SJ Impact Factor: 7.177*
*Volume 7 Issue VI, June 2019- Available at www.ijraset.com*

Table 1a: Summary of Vlasov's coefficients for the composite section.

| $a_{ij}=a_{ij}$ | $b_{ji}=b_{ji}$ | $Ck_j=Ck_j$ | $\gamma_{kk}=\gamma_{kk}$ |
|---|---|---|---|
| $a_{21}=0$ | $b_{21}=0$ | $C_{22}=16.34$ | |
| $a_{22}=165.695$ | $b_{22}=16.34$ | $C_{23}=-2.901$ | $\gamma_{12}=0$<br>$\gamma_{13}=0$ |
| $a_{23}=-1.247$ | $b_{23}=-2.901$ | $C_{24}=0$ | $\gamma_{14}=0$ |
| $a_{24}=0$ | $b_{24}=0$ | $C_{32}=-2.901$ | $\gamma_{22}=16.34$ |
| $a_{32}=-1.247$ | $b_{32}=-2.901$ | $C_{33}=16.016$ | $\gamma_{23}=-2.901$ |
| $a_{33}=3.465$ | $b_{33}=16.016$ | $C_{34}=0$ | $\gamma_{33}=16.016$ |
| $a_{34}=0$ | $b_{34}=0$ | | $\gamma_{34}=0$ |
| $s_{33}=0.0140xI_s$ | | | |

Table 1b: Summary of Vlasov's coefficients for the uniform concrete section.

| $a_{ij}=a_{ij}$ | $b_{ji}=b_{ji}$ | $Ck_j=Ck_j$ | $C_{ik}=C_{ik}=$ |
|---|---|---|---|
| $a_{21}=0$ | $b_{21}=0$ | $C_{21}=0$ | $C_{21}=0$ |
| $a_{22}=165.695$ | $b_{22}=16.34$ | $C_{22}=16.34$ | $C_{22}=16.34$ |
| $a_{23}=-0.002$ | $b_{23}=3.488$ | $C_{23}=3.488$ | $C_{23}=3.488$ |
| $a_{24}=0$ | $b_{24}=0$ | $C_{24}=0$ | $C_{24}=0$ |
| $a_{32}=-0.002$ | $b_{32}=3.488$ | $C_{32}=3.488$ | $C_{32}=3.488$ |
| $a_{33}=9.907$ | $b_{33}=12.514$ | $C_{32}=12.514$ | $C_{33}=12.514$ |
| $a_{34}=0$ | $b_{34}=0$ | $C_{34}=0$ | $C_{34}=0$ |
| $s_{33}=0.00953*I_s$ | | | |

## VIII. FLEXURAL-DISTORTIONAL ANALYSIS

A 60m span simply supported box girder structure whose cross section are shown in Fig.1(a) and 1(b) were considered. The loading was evaluated according to British specification for highway bridge live loads (BS5400-2-2006). The flexural and distortional components of the applied torsional load were computed according to BS5400-2-2006. Values obtained are, $\overline{q_2} = 665.36kN$, $\overline{q_3} = 64.92kN$. Where $\overline{q_2}$ and $\overline{q_3}$ are flexural and distortional components of the external work done on plate elements respectively. The governing equations for flexural-distortional analysis of single cell mono-symmetric box girder are given by eqns. (11) and (12).

Boundary conditions; For a simply supported box girder, we have the following boundary conditions; $V_2(0) = 0$, $V_2''(0) = 0$, $V_2(L) = 0$

$V_2''(L) = 0$, $V_3(0) = 0$, $V_3''(0) = 0$, $V_3(L) = 0$, $V_3''(L) = 0$

The relevant Vlasov coefficients obtained for the composite and non-composite sections are given in table 1(a and a);

Taking, $E_s = 200x10^9 N/m^2$, $E_c = 24x10^9 N/m^2$, $G_s = 80x10^9 N/m^2$ and $G_c = 9.6x10^9 N/m^2$,

k= $\frac{E}{G} = 2.5$, $\overline{q_2} = 665.36KN$, $\overline{q_3} = 755.73KN$, Substituting the Vlasov's coefficients into eqns.13(a-k), we obtain the coefficients of the governing differential equation summarized in table 2 for composite and uniform sections;

Table 2: Coefficients of the governing differential equation.

| Coefficients | Composite concrete–steel section | Uniform concrete section |
|---|---|---|
| $\alpha_1$ | 414.238 | 414.238 |
| $\alpha_2$ | -3.118 | -0.005 |
| $\alpha_3$ | -3.118 | -0.005 |
| $\alpha_4$ | 8.663 | 24.768 |
| $\beta_1$ | $5.558 \times 10^{-4}$ | $-1.193 \times 10^{-4}$ |
| $\beta_2$ | $7.281 \times 10^{-5}$ | $3.343 \times 10^{-5}$ |
| $\gamma_1$ | $-4.342 \times 10^{-5}$ | $-1.588 \times 10^{-5}$ |
| $K_1$ | $-6.044x\ 10^{-7}$ | $-1.844 x10^{-7}$ |
| $K_2$ | $-6.150 \times 10^{-7}$ | $-1.829 \times 10^{-7}$ |
| $K_3$ | $1.180 \times 10^{-5}$ | $3.141 \times 10^{-6}$ |
| $K_4$ | $-1.852 \times 10^{-6}$ | $-4.955x10^{-6}$ |

Substituting these coefficients into the governing eqns. (11) and (12), we obtain for the composite section;

$414.238V_2^{iv} - 3.118\ V_3^{iv} - 5.558\ x\ 10^{-4}V_2'' = 1.180x10^{-5}$ (16a)

and

$-3.118V_2^{iv} + 8.663V_3^{iv} - 7.281x10^{-5}V_3'' + 4.342\ x10^{-5}V_3 = 1.85 \times 10^{-6}$ (16b)

Solving eqns.16 (a & b) simultaneously by method of Fourier sine series and applying the boundary conditions, we obtain,

$V_2(x) = 4.520 \times 10^{-3} sin\frac{\pi x}{60}$ (17a)

$V_3(x) = 9.110 \times 10^{-2} \sin\frac{\pi x}{60}$ (17b)

For the non-composite section, we have,

$V_2(x) = 1.0120 \times 10^{-3} \sin\frac{\pi x}{60}$ (18a)

$V_3(x) = 24.50 \times 10^{-2} \sin\frac{\pi x}{60}$ (18b)

## IX. DISCUSSION OF RESULTS

The solution to the flexural- distortional equations of equilibrium for the composite section (eqns. 16a and 16b) is given by the expressions 17a and 17b. similarly the solution to the flexural- distortional equations of equilibrium for the non-composite section is given by the expressions 18a and 18b. They express the deformations of the 60m span simply supported study models.

Fig. 6 shows the variation of flexural displacement along the lengths of the composite and non-composite box girder sections, while Fig 7 presents the variation of distortional displacement along the lengths of the same sections.

The maximum (mid span) flexural displacements for the box girder sections are 4.52mm for the composite and 1.012mm for the non-composite section, while the maximum (mid span) distortional displacements are 91.1mm for the composite section and 24.500mm for the non-composite. From the results, the maximum flexural displacement for the composite section is 77.6% more than the maximum flexural displacement for the non-composite section. It also has 73.1% more distortional displacement when compared to the non-composite section. The results revealed that the non-composite section has a better flexural and distortional capacity than the composite section. Generally, it can be concluded that combining concrete and steel in a composite action in the arrangement shown in Fig.1a, does not enhance the flexural-distortional capacity of a box girder section, even though savings in weight and hence foundation cost can be achieved. That may explain why the use of composite (concrete-steel) box girder bridge is not a common practice, as reinforced concrete box girder bridge predominates.

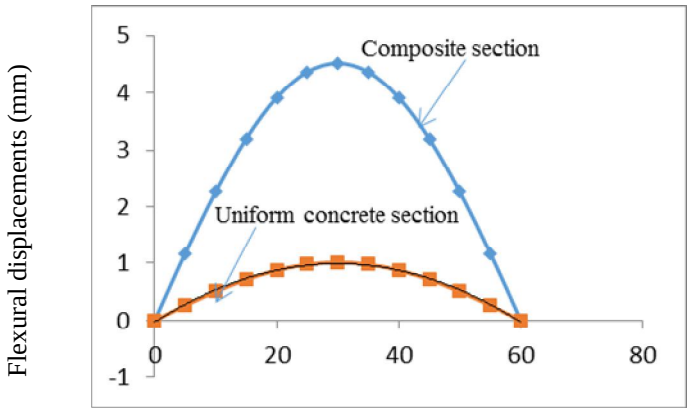


Fig. 6: Variation of flexural deformation along the length of the girder sections

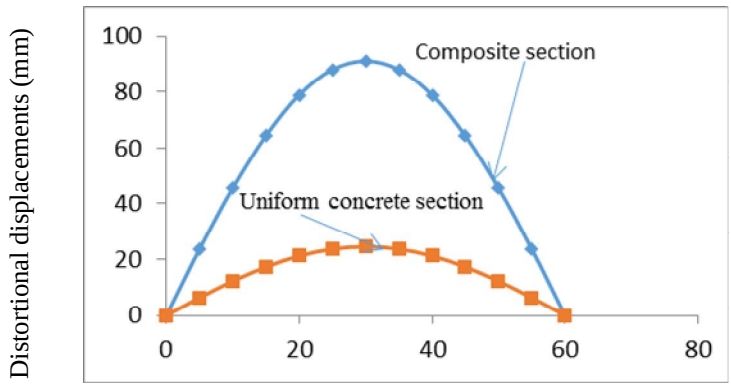


Fig. 7: Variation of distortional deformation along the length of the girder sections

## X. CONCLUSION

Equations (11) and (12) are the governing differential equations of equilibrium for flexural-distortional analyses of a mono-symmetric box girder section, while expressions 17(a and b) and 18(a and b) are the solutions to the governing equations for the composite and the non-composite sections respectively. The study shows that the non-composite section has the capacity to resist flexural and distortional deformations more than the composite section in the arrangement considered, i.e. the top and bottom flanges made of concrete and the webs made of steel.

It therefore follows that savings in the weight of materials and hence the cost of foundation in composite section, results to loss of flexural and distortional stabilities.

## REFERENCE

[1] Shital C. Chaudhari and Satish K. Deshmukh (2016), Effect of orthotropy on distortional behaviour of laminated composite trapezoidal box girder, International Journal of Pure and Applied Research in Engineering, Vol.5(2):236-250.
[2] Shetty M.S. (2010), Concrete Technology, S Chand and Company ltd, New Delhi.
[3] Mosley B. et al (2007), Reinforced Concrete Design, Book Power Publishers London.
[4] Mizuguchi K., Ashiduka, K, Yoda T. Sato K., Sakurada M. and Hidaka S. (1998(, Loading Test of Hondani Bridge, Bridge Found Eng., 32(10) 25-34.
[5] Matsui T., Tategami H„ Ebina T., Tamura, S. and Ogawa M. (2006), A vibration Characteristics and Main Girder Rigidity Evaluation Method. Second Fib Congress, Naplos, Italy 1-11.
[6] Shitou K., Nakazono A., Suzuki N., Nagamoto N. and Asai H. (2008), Experimental Research on Shear behaviour of Corrugated Steel web bridge. Proc. A Tapan Soc. Civ, Eng 64 (2) 223-234.
[7] Ding Y, Jiang K. B. and Lim Y.W. (2012). Non Linear Analysis for PC Box Girder with Corrugated Steel Web, Thin-Walled Struct., 51, 167- 173.
[8] Sennah, K.M., Khaled and Kennedy J.B., (2003). Design for shear in curved Composite multiple steel box girder bridges" Journal of Bridge Engineering, Vol.8, P l44-152.
[9] Gupta P.K., Singh K., and Mishra A., (2010). Parametric study on behavior of box girder bridges, using finite element method, Asian journal of civil engineering, vol. 11, no.l, pp 135-148'
[10] Sayed-Ahmed E.Y (2007), Design Aspect of Steel I-girder with Corrugated Steel Webs J. Struct Eng. 27-40.
[11] Okeil, A.M., and EI-Tawil, S. (2004). "Warping stresses in curved box girder bridges: Case study". Journal of Bridge Engineering, vol.9, issue 5, p.487- 496.
[12] Kollar L.P and Springer, (2003), Mechanics of Composite Structures, Cambridge University Press.
[13] Kollar L.P. and Pluzsik A. (2002) Analysis of Thin Walled Composite Beams with arbitrary layup, Journal of Reinforced Plastics and Composites Vol. 21, P. 1423 - 1465.
[14] Martin A. (2003, Finite Element Modeling of Composite Bridge Stability, Msc Thesis, Royal Institute of Tech. Stockholm Siveden.
[15] Sarode B. Ashish and Vesmawala G.R., (2014), "parametric study of horizontally curved box girders for torsional behavior and stability". International refereed journal of engineering and sciences (IRJES), vol. 3, issue 2, pp 50 -55
[16] Osadebe N.N. and Chidolue, C.A. (2012), Tortional-distortional response of thin-walled mono symmetric box girder structures, International Journal of Engineering Research and Application, vol.2, issue 3, pp 814-821
[17] Osadebe N.N. and Chidolue, C.A. (2012), flexural-distortional performance of thin-walled mono symmetric box girder structures, International Journal of Engineering Research and Technology, vol.1, issue 4, June 2012.
[18] Varbernov, C.P. (1976), Theory of Elasticity, Techntka Press Sofia, 4th edition, p.254-271Vlasov,
[19] Vlasov V.Z. (1961). "Thin walled elastic beams", 2nd Ed., National Science Foundation, Washington, D.C.
[20] Vlasov V.Z. (1958). "Thin walled space structures" Gosstrojizdat, Moscow.
[21] Rekach V.G, Static theory of thin-walled space structures, MIR Publishers, Mosco (1978).

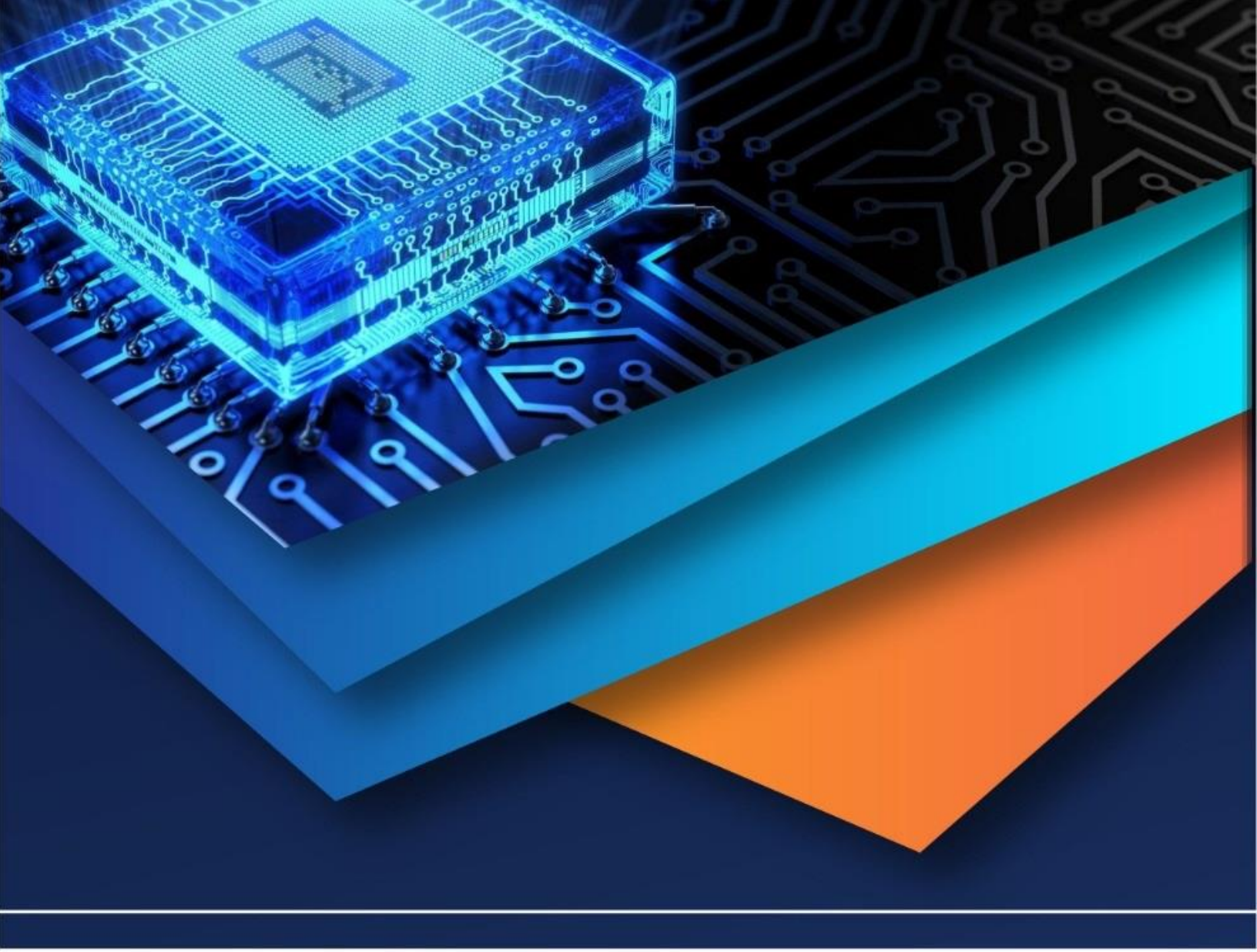

10.22214/IJRASET

45.98

IMPACT FACTOR: 7.129

IMPACT FACTOR: 7.429

# INTERNATIONAL JOURNAL FOR RESEARCH

IN APPLIED SCIENCE & ENGINEERING TECHNOLOGY